

## Supporting information

# The Influence of Chloride Ions on the Synthesis of Colloidal Branched CdSe/CdS Nanocrystals by Seeded Growth

*Mee Rahn Kim, Karol Miszta, Mauro Povia, Rosaria Brescia, Sotirios Christodoulou, Mirko Prato, Sergio Marras, and Liberato Manna\**

Istituto Italiano di Tecnologia, Via Morego 30, 16163 Genova, Italy

\* To whom correspondence should be addressed: [liberato.manna@iit.it](mailto:liberato.manna@iit.it)

## Experimental Details of syntheses

**Table 1.** Summary of reagent amounts involved in the syntheses of NCs.

Samples	CdO (mmol)	CdCl <sub>2</sub> (mmol)	ODPA (mg)	HPA (mg)	PPA (mg)
Figure 1a	0.50	0.00	290	80	0
Figure 1c	0.49	0.01	290	80	0
Figure 1d	0.48	0.02	290	80	0
Figure 1e (left panels of Figure 2)	0.47	0.03	290	80	0
Figure 1f (right panels of Figure 2, Figure 3)	0.34	0.16	290	80	0
Figure 4b (Figure S18b)	0.47	0.03	251	100	0
Figure 4c (Figure S18f)	0.47	0.03	290	0	60
Figure 4d (Figure S18k)	0.47	0.03	305	38	25
Figure S1a	0.50	0.00	290	80	0
Figure S1b	0.47	0.03	290	80	0
Figure S10a	0.50	0.00	290	80	0
Figure S10b	0.49	0.01	290	80	0
Figure S10c	0.34	0.16	290	80	0
Figure S11a	0.50	0.00	290	80	0
Figure S11b	0.49	0.01	290	80	0
Figure S11c	0.34	0.16	290	80	0
Figure S12a	0.50	0.00	360	110	3.4
Figure S12b	0.50	0.00	580	160	5.4
Figure S13a	0.50	0.00	290	0	60
Figure S13b	0.50	0.00	350	0	40
Figure S13c	0.50	0.00	0	0	40 with 290 mg TDPA <sup>a)</sup>
Figure S13d	0.50	0.00	0	50 with 250 mg TDPA	0
Figure S14a-c	0.50	0.00	290	80	0
Figure S15	0.47 with 3.4 $\mu$ L of HCl	0.00	290	80	0
Figure S16	0.47 with 10 mg of NaCl	0.00	290	80	0
Figure S17a	0.47	0.03	450	0	0
Figure S17b	0.47	0.03	0	225	0
Figure S17c	0.47	0.03	0	0	167
Figure S18a	0.47	0.03	223	108	0

Figure S18b (Figure 4b)	0.47	0.03	251	100	0
Figure S18c	0.47	0.03	290	38	30
Figure S18d	0.47	0.03	275	85	0
Figure S18e	0.47	0.03	233	10	73
Figure S18f (Figure 4c)	0.47	0.03	290	0	60
Figure S18g	0.47	0.03	251	0	73
Figure S18h	0.47	0.03	251	11	65
Figure S18i	0.47	0.03	275	45	30
Figure S18j	0.47	0.03	258	20	48
Figure S18k (Figure 4d)	0.47	0.03	305	38	25

<sup>a)</sup> TDPA: *tetra*-decylphosphonic acid

## Results of syntheses carried out at various molar fractions of CdCl<sub>2</sub>

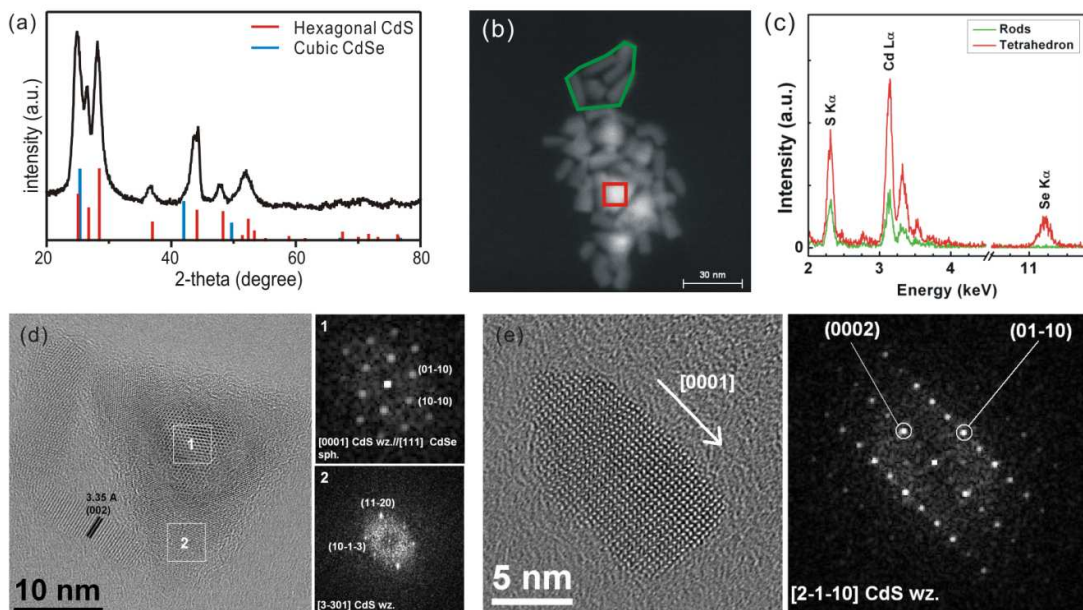


**Figure S1.** Results of syntheses carried out in absence of CdCl<sub>2</sub>. (a) XRD pattern: the strong diffraction peaks can be ascribed to wurtzite CdS, while weak diffraction peaks corresponding to the sphalerite CdSe can be identified; (b) STEM-HAADF image of a group of nanoparticles and (c) corresponding EDS analyses of two regions indicated in panel (b): the EDS spectrum acquired over a group of nanorods (green) shows an atomic composition Cd:S:Se = 52:48:0, while for the central area of a tetrahedron (red) the atomic composition is Cd:S:Se = 51:32:17; (d) HRTEM image and Fourier transform (FT) of selected regions in a tetrahedral shaped core-shell CdSe/CdS NCs: the FE marked as 1 designates wurtzite CdS and sphalerite CdSe whereas that marked as 2 indicates only wurtzite CdS; (e) HRTEM image and corresponding FT of a nanorod of wurtzite CdS.

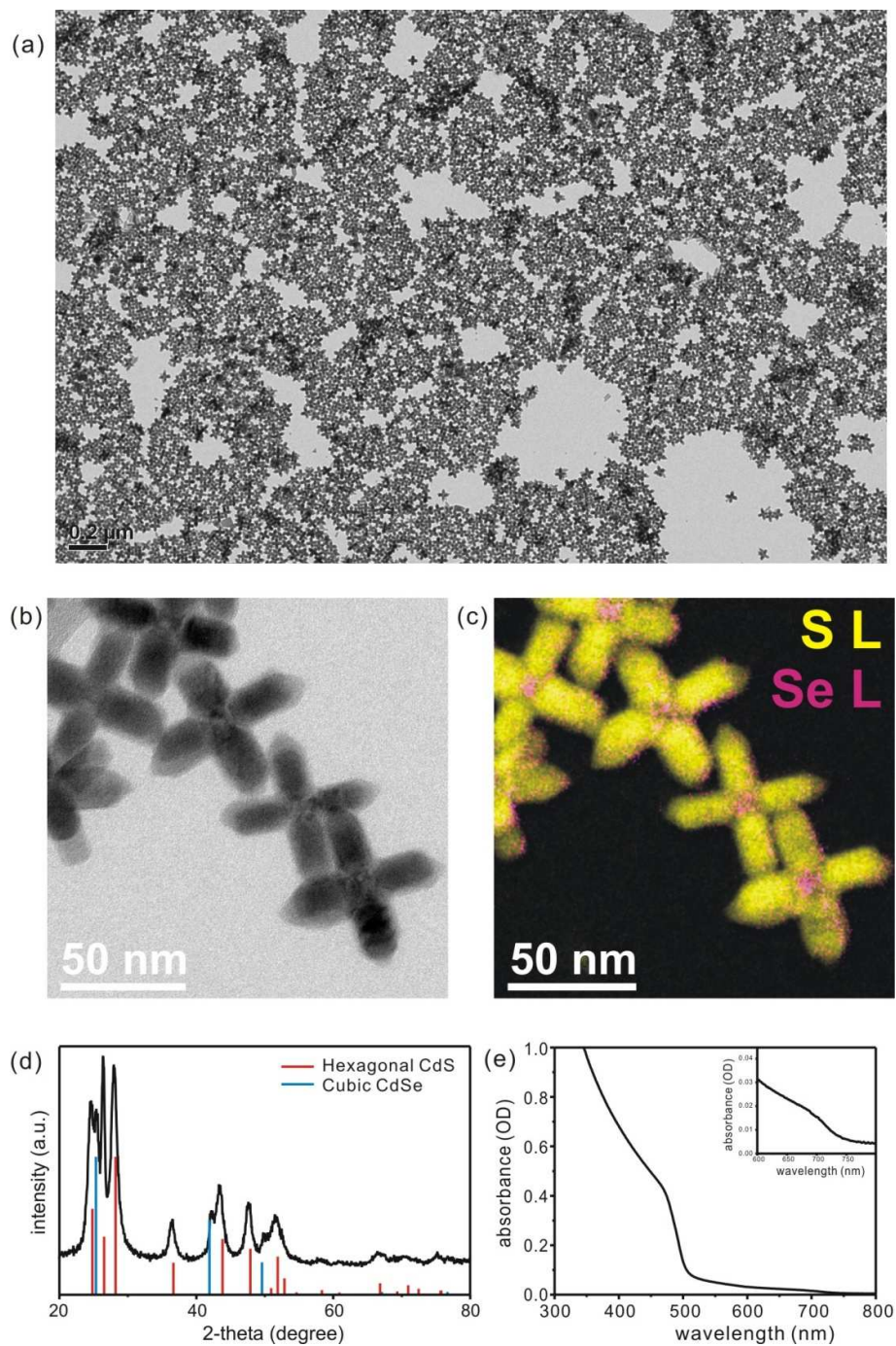


**Figure S2.** Results of synthesis carried out with  $f_{\text{CdCl}_2} = 0.06$ . (a) Overview TEM image of several CdSe/CdS octapods, obtained directly from the synthesis, without size-selective precipitation, highlighting their shape and size monodispersity; (b) zero-loss TEM image of a small group of particles and (c) corresponding composition of EFTEM elemental maps for S (yellow) and Se (magenta): the elemental analysis confirms the CdSe and CdS nature of the core and the pods, respectively; (d) XRD pattern, showing peaks ascribable to both wurtzite CdS

and sphalerite CdSe; (e) UV-vis spectrum, indicating absorbance of CdS at  $\sim 500$  nm and that of CdSe at  $\sim 700$  nm . Optical absorption measurements of NCs dispersed in toluene were carried out using a Varian Cary 5000 UV-Vis-NIR spectrophotometer.

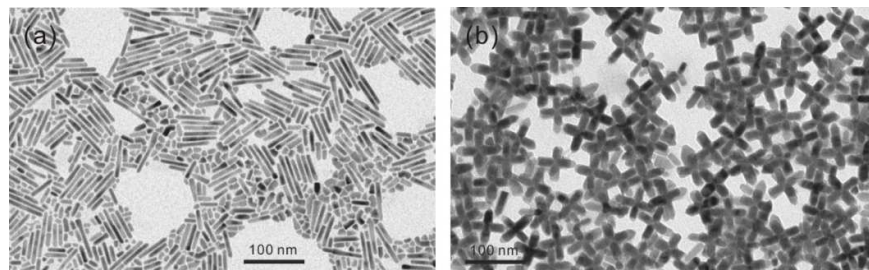


**Figure S3.** TEM images of NCs formed via the two-step approach (first CdSe NCs were prepared by cation exchange from  $\text{Cu}_{2-x}\text{Se}$  NCs, then these were injected together with TOPS in the flask). In (a) no  $\text{CdCl}_2$  was added ( $f_{\text{CdCl}_2} = 0.00$ ), while in (b)  $f_{\text{CdCl}_2}$  was equal to 0.06 (see main text). Nanorods and irregularly shaped NCs were synthesized in the first case, while octapod-shaped NCs were synthesized in the second case. Therefore, the results obtained with the two-step approach are comparable to those obtained with the one-step approach described in the main text. In both cases the syntheses were run for 10 min.

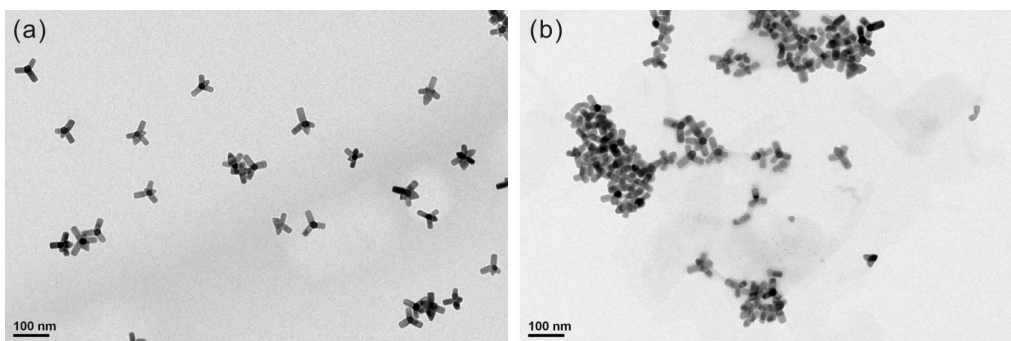


**Figure S4.** TEM images of NCs synthesized with  $f_{\text{CdCl}_2} = 0.50$ . Aliquots are taken at (a) 5 min and (b) 10 min.

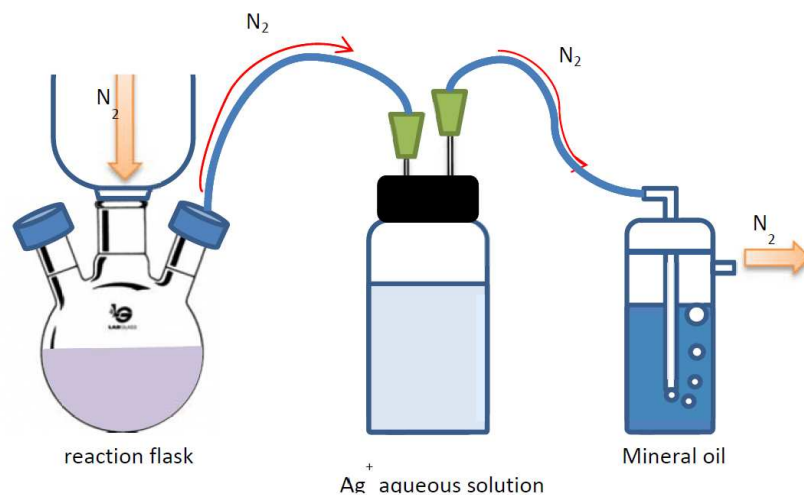


**Figure S5.** In this control experiment, 0.12 g of  $\text{CdCl}_2$  were added into a reaction flask containing 3.0 g of TOPO and 0.23 g of HPA. The flask was then heated up to 380 °C under  $\text{N}_2(\text{g})$  flow. If HCl vapors would develop upon heating, a precipitate of  $\text{AgCl}$  would form in the vial containing the  $\text{Ag}^+$ -aqueous solution. This solution however remained clear and colorless. Therefore, no HCl was freed in this case and all Cl species remained in the flask.

### Shape evolution

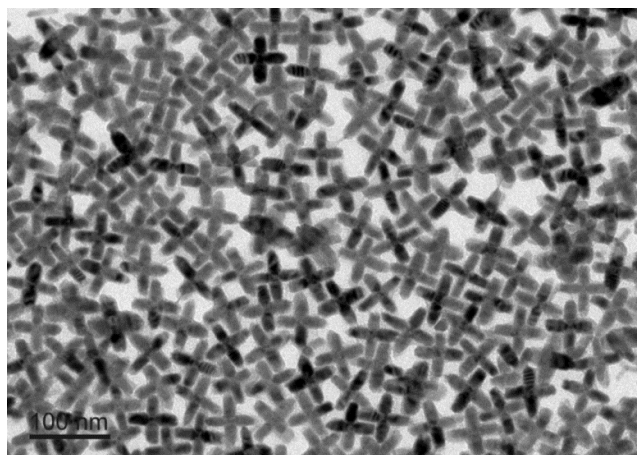


**Figure S6.** Control experiment. TEM image of octapod-shaped NCs synthesized with  $f_{\text{CdCl}_2} = 0.06$ . In this case, the synthesis reaction was run for 1 hour, instead of 10 minutes. However, the NCs, which formed early during the synthesis, did not suffer shape evolution over all this time.

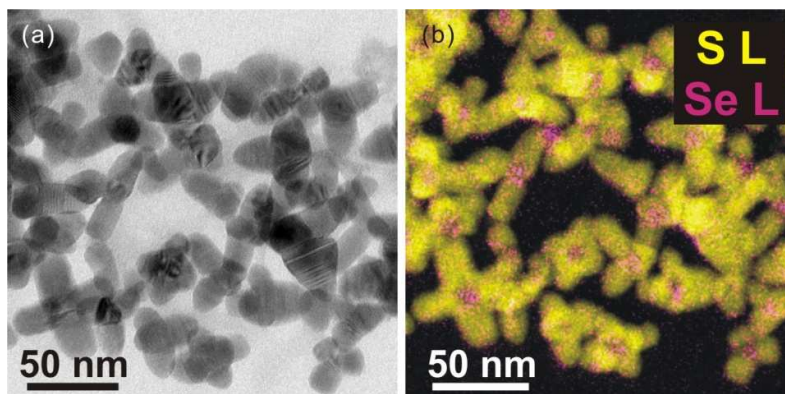


**Figure S7.** (a) Zero-loss TEM and (b) corresponding combination of EFTEM elemental maps for S (yellow) and Se (magenta) for a group of NCs synthesized with  $f_{CdCl_2} = 0.32$ .

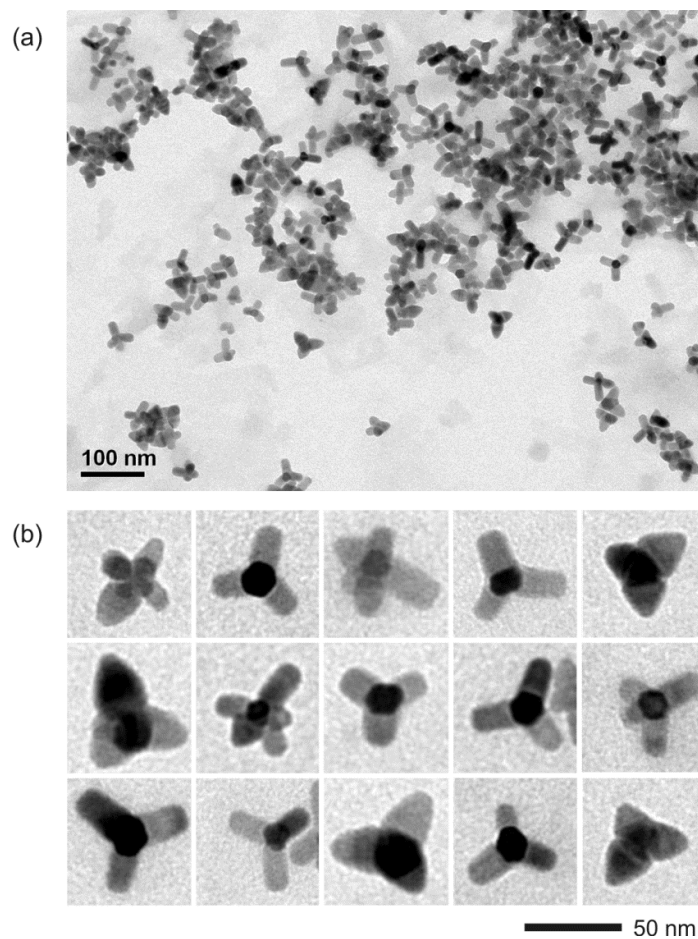


**Figure S8.** (a) Low magnification and (b) high magnification TEM images of several NCs in an aliquot of the synthesis carried out at  $f_{CdCl_2} = 0.32$  (see Figure 3 of the main text) taken 5 min after the injection.

## Detection of Cl-species in the final samples

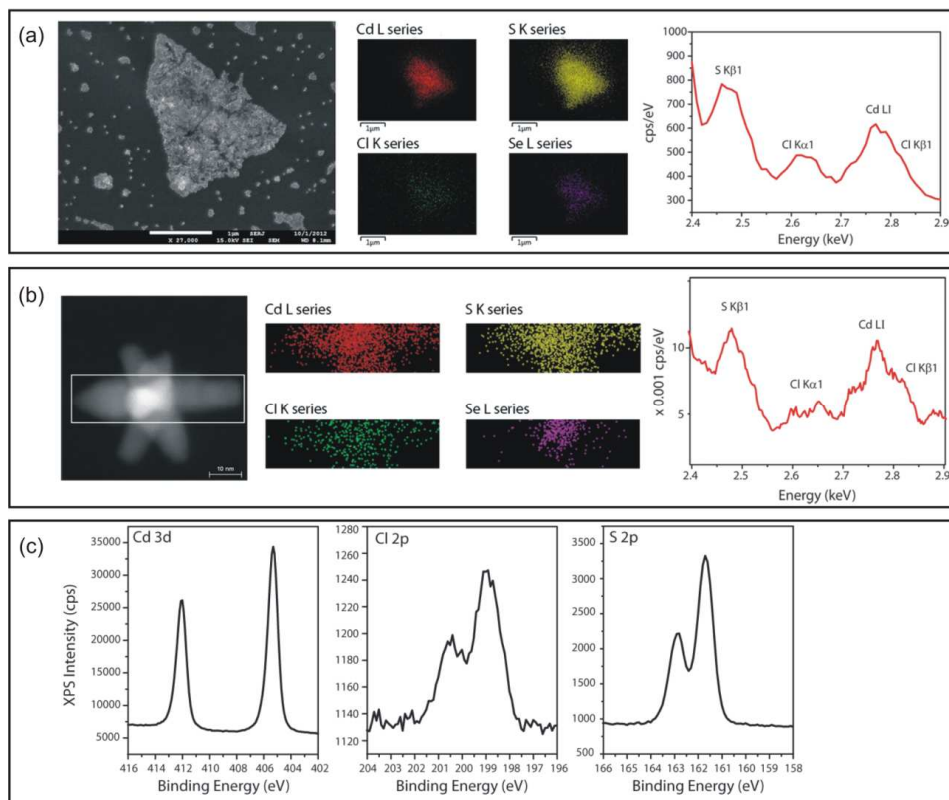


**Figure S9.** Detecting the presence of Cl species in samples NCs obtained at  $f_{CdCl_2} = 0.32$  at 1 minute after seed injection, after thorough washing. (a) (left) HRSEM image of NCs on an amorphous carbon substrate and (middle, right) related EDS elemental maps and spectrum: a weak signal of chlorine is clearly associated with a group of NCs; (b) (left) HRTEM image of a single octapod and (middle, right) corresponding EDS elemental maps and EDS spectrum averaged every 13 points: although the signals are very weak, the analyses indicate the evidence of chlorine; (c) XPS narrow scans on Cd 3d, Cl 2p and S 2p peaks: the signal of Cl is clearly visible and the position of Cl 2p $_{3/2}$  peak at  $(199.0 \pm 0.2)$  eV is consistent with the presence of CdCl $_2$  in the sample (A. V. Naumkin, A. Kraut-Vass, S. W. Gaarenstroom, and C. J. Powell, NIST X-ray Photoelectron Spectroscopy Database, <http://srdata.nist.gov/xps/>). Cd 3d $_{5/2}$  at  $(405.3 \pm 0.2)$  eV and S 2p $_{3/2}$  at  $(161.7 \pm 0.2)$  eV are typical for CdS (NIST). This might either indicate Cl species directly bound to the surface Cd atoms of the NCs, or residual CdCl $_2$  present as separate crystals (which however we could not detect by other techniques), or yet residual complexes involving Cd $^{2+}$  and Cl $^-$  ions. The sample was however carefully cleaned. Concerning the quantitative chloride analyses, the atomic composition from HRSEM-and HRTEM-EDS is Cd:Cl=98:2 and that from surface-sensitive XPS is Cd:Cl=96:4.

## Control syntheses

### 1. CdS and CdSe NCs synthesized in absence of seeds

In order to explore our hypothesis on the influence of Cl<sup>-</sup> ions on nucleation and growth, syntheses were carried out in the absence of CdSe seeds and with variable  $f_{\text{CdCl}_2}$  values (Figure S10). The observed morphologies of the resulting CdS NCs at 10 minutes after injection of TOPS are strongly dependent on  $f_{\text{CdCl}_2}$ . Small CdS nanospheres (diameter: 6 nm) were formed in the Cl<sup>-</sup>-free reaction environment ( $f_{\text{CdCl}_2} = 0.00$ ). On the other hand, CdS nanorods (diameter: 9 nm, length: 33 nm) and bullet-shaped CdS nanocrystals (diameter: 55 nm, length: 140 nm) were formed in the reaction flasks with  $f_{\text{CdCl}_2} = 0.02$  and  $f_{\text{CdCl}_2} = 0.32$ , respectively. In addition, the NC concentrations of the resulting products were:  $1.02 \times 10^{-5}$  M for small CdS nanospheres,  $4.12 \times 10^{-7}$  M for CdS nanorods, and  $3.95 \times 10^{-9}$  M for bullet-shaped CdS nanocrystals.

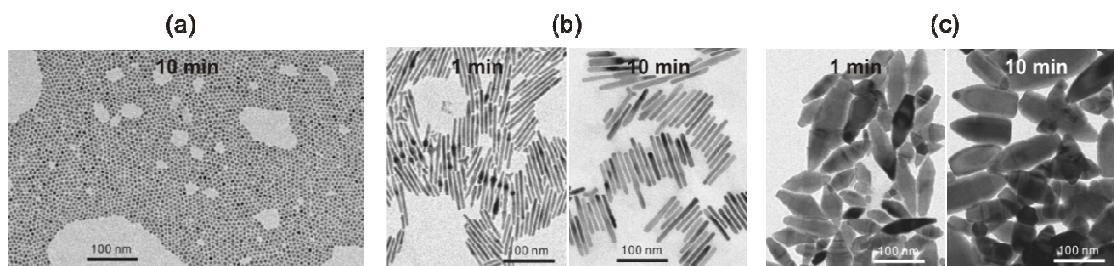


**Figure S10.** TEM images of (a) CdS nanospheres, (b) CdS nanorods, and (c) CdS nanobullets synthesized in absence of  $\text{Cu}_{2-x}\text{Se}$  seeds with  $f_{\text{CdCl}_2}$  equal to 0.00 (a), 0.02 (b), and 0.32 (c), respectively. (b) and (c) show CdS NC aliquots taken at 1 minute (left panel) and 10 minutes (right panel) after injection. The reaction time is indicated in each panel.

When TOPS is replaced by TOPSe, the observed morphologies of CdSe NCs (Figure S11) synthesized in absence of seeds are also strongly dependent on  $f_{\text{CdCl}_2}$ . The small elongated CdSe NCs in Figure S11a (diameter: 11 nm, length: 23 nm) and in Figure S11b (diameter: 13 nm, length: 21 nm) were formed in the reaction environments with  $f_{\text{CdCl}_2} = 0.00$

and  $f_{\text{CdCl}_2} = 0.02$ , respectively. On the other hand, diamond-shaped CdSe NCs (diameter: 42 nm, length: 52 nm) in Figure S11c were formed in a reaction flask with  $f_{\text{CdCl}_2} = 0.32$ . In addition, the NC concentrations of the resulting products were:  $5.65 \times 10^{-8}$  M for CdSe NCs in Figure S11a,  $4.80 \times 10^{-8}$  M for CdSe NCs in Figure S11b, and  $2.04 \times 10^{-9}$  M for diamond-shaped CdSe nanocrystals in Figure S11c. By XRD, all these samples had wurtzite structure.

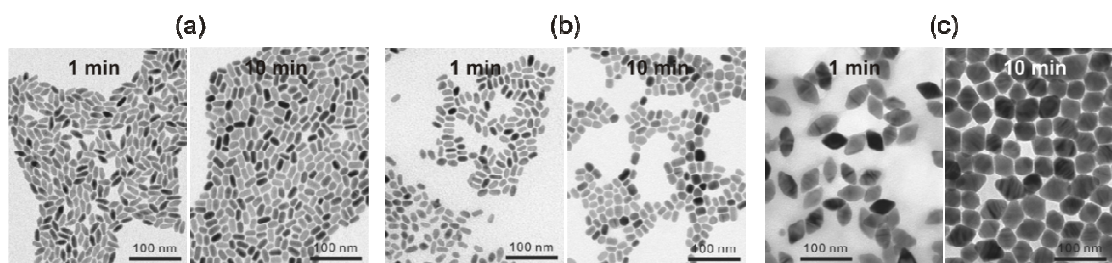


**Figure S11.** TEM images of CdSe NCs synthesized in absence of  $\text{Cu}_{2-x}\text{Se}$  seeds and by adding TOPSe instead of TOPS, at (a)  $f_{\text{CdCl}_2} = 0.00$ , (b)  $f_{\text{CdCl}_2} = 0.02$ , and (c)  $f_{\text{CdCl}_2} = 0.32$ . The reaction time is indicated in each panel.

## 2. Attempt to grow octapods using higher alkylphosphonic acid:Cd ratios

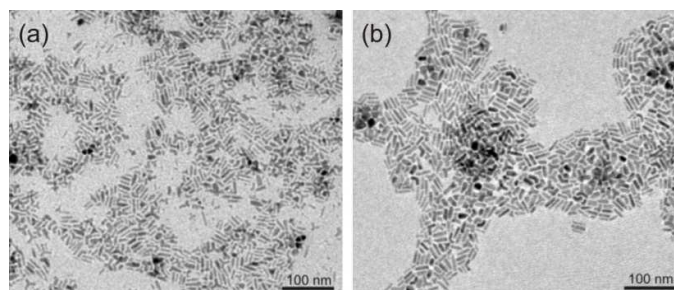


**Figure S12.** TEM images of resulting NCs prepared by no addition of  $\text{CdCl}_2$ , ( $f_{\text{CdCl}_2} = 0.00$ ) but by using alkylphosphonic acid:Cd ratios of (a) 3.4:1 and (b) 5.4:1, respectively, instead of of 2.7:1 as used for various syntheses of octapods described in the main text. The reaction was performed at 380 °C.

### 3. Using phosphonic acids with shorter alkyl chains

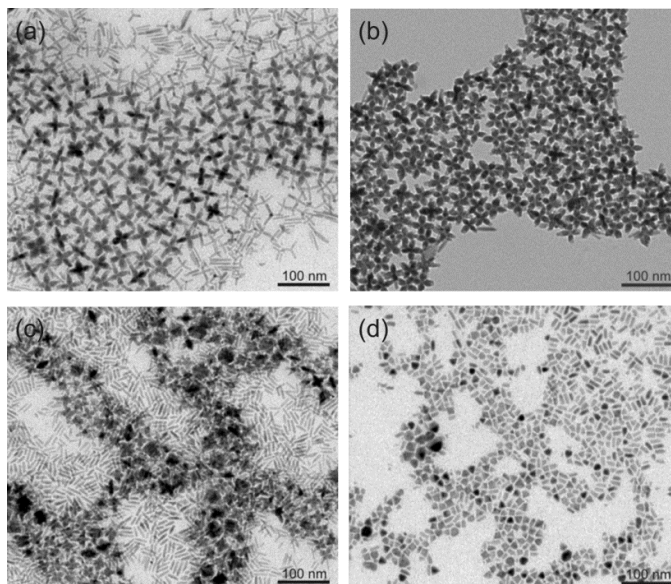


**Figure S13.** TEM images of resulting NCs prepared by no addition of  $\text{CdCl}_2$ , ( $f_{\text{CdCl}_2} = 0.00$ ) but by using a mixture of several alkylphosphonic acids of (a,b) ODPA and PPA: the weight percentages of PPA over ODPA are 21wt% and 11wt%, respectively; (c) TDPA and PPA: the weight percentage of PPA over TDPA is 14wt%; and (d) TDPA and HPA: the weight percentage of HPA over TDPA is 20wt%. In all these experiments, the ratio of alkylphosphonic acid to Cd is fixed as 2.7:1. Either side nucleation of other shapes cannot be avoided, or irregularly shaped NCs are the main product, or octapods have pods often ending with very sharp tips (b-c).

### 4. Different reaction temperatures

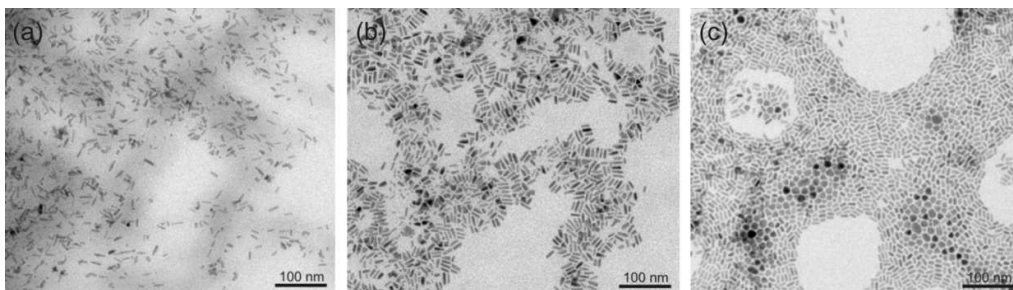


**Figure S14.** TEM images of resulting NCs prepared by no addition of  $\text{CdCl}_2$ , ( $f_{\text{CdCl}_2} = 0.00$ ) but by working at reaction temperatures different from 380°C: (a) 320 °C, (b) 350 °C, and (c) 410 °C.



## 5. Using alternative chlorine sources

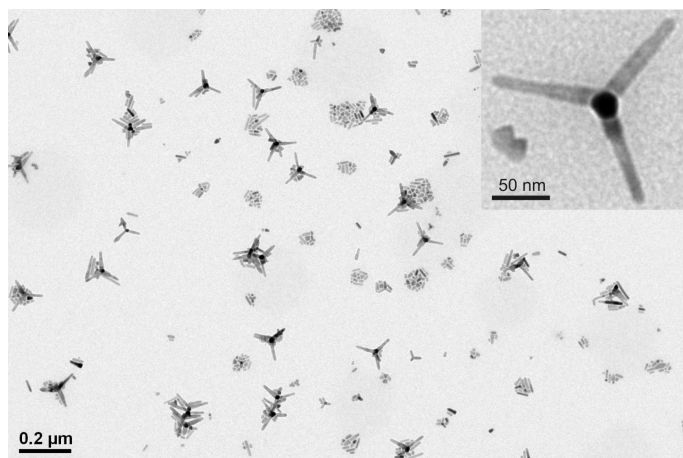


**Figure S15.** TEM image of NCs synthesized by using 3.4 μL of HCl as a chlorine source instead of CdCl<sub>2</sub>.

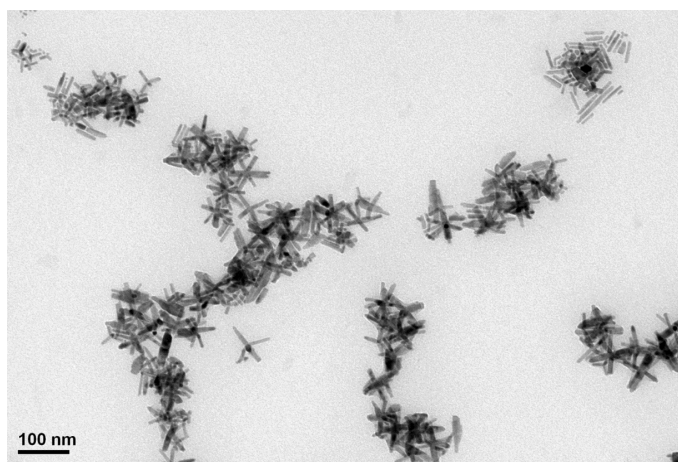


**Figure S16.** TEM image of nanocrystals synthesized by using 10 mg of NaCl as a chlorine source instead of CdCl<sub>2</sub>.

## Tuning the length of the

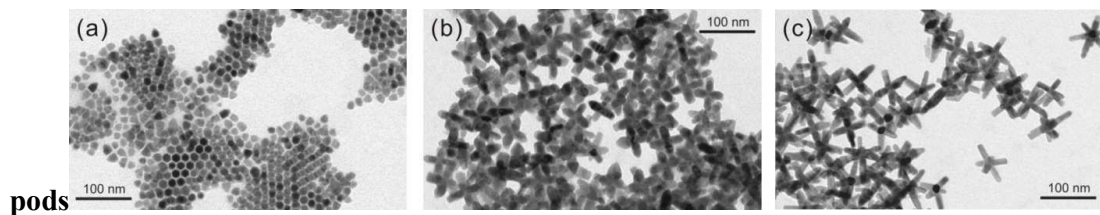


**Figure S17.** TEM images of CdSe/Cds NCs synthesized by using a single phosphonic acid, at : (a) ODPA, (b) HPA, and (c) PPA. In all the syntheses,  $f_{CdCl_2}$  was equal to 0.06.

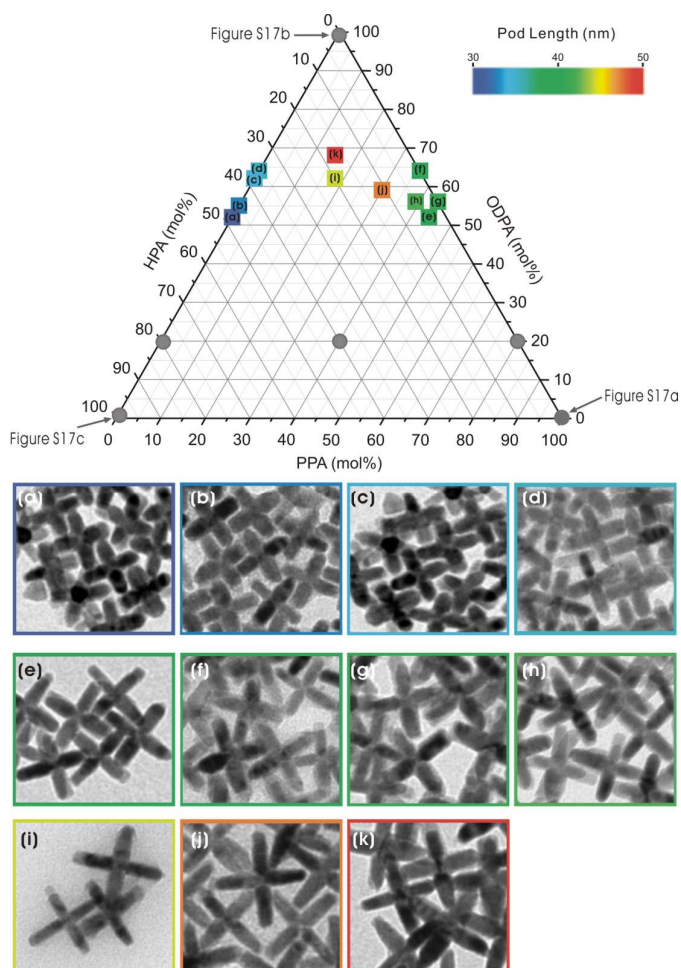


**Figure S18.** Top: Schematic diagram of the outcome of the experiments performed by varying the relative amounts of three different alkyl phosphonic acids (PPA, HPA and ODPA), while keeping constant the ratio of total moles of phosphonic acids to moles of Cd (2.7:1) and also  $f_{CdCl_2}$  (0.06). In these experiments we could fine tune the pod lengths of the octapods. Bottom (a-k): corresponding TEM images of the obtained octapods,

having diverse pod lengths and ranging from 30 nm to 50 nm. Representative TEM images corresponding to the samples prepared using only PPA, only HPA or only ODPA, ie. at the corners of the diagram, are actually reported in Figure S17.